Efficiency promotion for an on-ramp system based on intelligent transportation system information*

Xie Dong-Fan(谢东繁)†, Gao Zi-You(高自友), and Zhao Xiao-Mei(赵小梅)

School of Traffic and Transportation, Beijing Jiaotong University, Beijing 100044, *China*

(Received 2 November 2009; revised manuscript received 22 March 2010)

The effect of cars with intelligent transportation systems (ITSs) on traffic flow near an on-ramp is investigated by car-following simulations. By numerical simulations, the dependences of flux on the inflow rate are investigated for various proportions of cars with ITSs. The phase diagrams as well as the spatiotemporal diagrams are presented to show different traffic flow states on the main road and the on-ramp. The results show that the saturated flux on the main road increases and the free flow region is enlarged with the increase of the proportion of cars with ITS. Interestingly, the congested regions of the main road disappear completely when the proportion is larger than a critical value. Further investigation shows that the capacity of the on-ramp system can be promoted by 13% by using the ITS information, and the saturated flux on the on-ramp can be kept at an appropriate value by adjusting the proportion of cars with ITS.

Keywords: traffic flow, car-following model, ITS information, on-ramp

PACC: 0550, 0520, 0570F, 0570J

1. Introduction

Traffic congestion is serious in most of the large cities all over the world. To uncover the mechanism of various phenomena appearing in traffic flow, lots of studies have been conducted with different traffic models, such as the car-following model, cellular automaton model, hydrodynamic model and gas kinetic model.[1,2] Car-following model is one of the most important microscopic models. It depicts the motion of cars by differential equations and thus is appropriate for theoretical analysis and numerical simulations. In 1995, Bando *et al.*[3] proposed the optimal velocity (OV) model. Since it is simple and capable of reproducing many nonlinear characteristics of traffic flow, such as nonequilibrium traffic flow, jam formation and stop and go waves, much attention has been attracted and some extensions have also been presented.[4−7]

In order to suppress traffic jams and promote the efficiency of road systems, many approaches to traffic control systems are introduced. Recently, with the development of intelligent transportation system (ITS),the traffic control system has been utilized as a part of ITS, and for the cars equipped with the ITS the drivers can receive the information about adjacent cars on roads. Several traffic flow models have been proposed by taking into account the ITS information.[8−17] Some researches focus on the effect of multiple headways of preceding or following cars,[8−14] and others focus on the effect of velocity difference on traffic flow.[15,16] The results indicate that the ITS information about headway or the velocity difference can stabilize the traffic flow. In addition, Xie *et al.*[17] have presented the extended car-following model by simultaneously introducing both multiple headways and velocity difference of preceding cars, and indicate that traffic flow can be stabler.

On the other hand, the adaptive cruise control (ACC) system allows a car to follow another one at an appropriate speed and distance automatically. The ACC cars can be realized by the cars with ITSs. Some work has been done on the effect of the ACC system on the traffic flow.[18−30] The effect of the ACC vehicle on traffic flow stability is widely studied.[18−22] Treiber and Helbing[23] and Kesting *et al.*[24] reported that nearly all of the congestions were eliminated if 20% of vehicles were equipped with the ACC systems. Davis[25] showed that the ACC system could suppress wide moving jams. He also proposed a cooperative merging for ACC vehicles to improve throughput.[26]

*Project partially supported by the National Basic Research Program of China (Grant No. 2006CB705500), the National Natural Science Foundation of China (Grant Nos. 70631001 and 70701004), and the Innovation Foundation of Science and Technology for Excellent Doctorial Candidate of Beijing Jiaotong University (Grant No. 141046522).

†Corresponding author. E-mail: dongfanxie@gmail.com

© 2010 Chinese Physical Society and IOP Publishing Ltd

VanderWerf *et al.*[27] specifically considered the effect of ACC vehicle on highway capacity. Ioannou and Stefanovic[28] analysed mixed traffic, considering the effects of unwanted cut-ins due to larger gaps in front of ACC cars.

Since congestion usually occurs at bottlenecks, the effect of ITS information on traffic flow should therefore be investigated. The purpose of the present work is to show the effect of ITS information on the phase transition in traffic flow and the capacity of the on-ramp system. In this paper, numerical simulations are used to investigate the on-ramp system. The OV model and the multiple headway and velocity difference (MHVD) model are used to depict the motion of cars with and without ITSs, respectively. The fluxes and the phase characteristics are investigated for various proportions of cars with ITSs. The results show that the free flow region of the main road can be enlarged, and the saturated flux increases with the increase of the proportion of cars with ITSs. Also, the capacity of on-ramp system can be promoted by introducing the ITS.

The remaining part of this paper is organized as follows. In Section 2, the OV model and the MHVD model are reviewed, and the merging rules near the on-ramp are also introduced. In Section 3, numerical simulations are performed and the results and discussions are given. Conclusions are drawn in Section 4.

2. Model

On-ramps are typical traffic bottlenecks which usually induce traffic jams. Figure 1 shows the sketch of an on-ramp system. As shown in the figure, both the main road (lane 1) and the on-ramp share one lane. The on-ramp system consists of five sections: A, B, C, C1 and D. Sections A and B are the main road and the on-ramp upstream of the merging region, respectively. Section C on the main road is the merging region, where cars from section C1 on the ramp are interwoven with those from upstream main road. Merging cars changing from section C1 to section C are performed as long as the safe conditions are satisfied. Section D is the main road downstream of the merging region. There are two types of cars, i.e. cars with and without ITS. They have the same sizes and maximum velocities. However, their dynamical behaviours are different. The famous OV model widely used in traffic flow simulations is selected to depict the motion of cars without ITSs. The MHVD model, in which the multiple ITS information (multiple headways and velocity difference) about preceding cars is considered, is used to depict the motion of cars with ITSs.

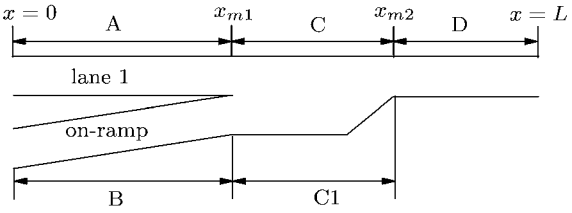


Fig. 1. Sketch of the on-ramp system in simulation.

2.1. Optimal velocity (OV) model

The dynamics of cars without ITSs is described by the OV model, in which it is assumed that each car has a legal velocity, which depends on the headway in the OV model. The dynamical equation of the OV model is given as[3]

$$\frac{\mathrm{d}^2 x_n(t)}{\mathrm{d}t^2} = a[V(\Delta x_n(t)) - v_n(t)], \quad (n = 1, 2, \ldots, N), \tag{1}$$

where $a = 1/\tau$ is the sensitivity of the driver, N is the total number of cars, $x_n(t)$ and $v_n(t)$ are the position and the velocity of car n at time t, $\Delta x_n(t)$ is the headway of car n at time t, $V(\cdot)$ is the optimal velocity function and the following form proposed by Helbing and Tilth[4] is chosen,

$$V(\Delta x_n(t)) = V_1 + V_2 \tanh(C_1(\Delta x_n(t) - l_c) - C_2), \tag{2}$$

where l_c is the average length of cars and it is assumed to be 5 m in the simulation. The parameter values are $V_1 = 6.75$ m/s, $V_2 = 7.91$ m/s, $C_1 = 0.13$ m^{-1}, and $C_2 = 1.57$.

2.2. Multiple headway and velocity difference (MHVD) model

Intelligent transportation system (ITS) has been adopted in some big cities. When ITS offers local traffic information, traffic congestions can be alleviated. By taking into account the ITS information about multiple preceding cars, the MHVD model is proposed based on the OV model and its extended models.[17] The MHVD model is used to depict the motion of cars with ITSs and the dynamical equation is

$$\frac{\mathrm{d}^2 x_n(t)}{\mathrm{d}t^2} = a[V(\Delta x_n(t), \Delta x_{n+1}(t), \ldots, \Delta x_{n+p-1}(t)) - v_n(t)] + \sum_{j=1}^{q} \kappa_j \Delta v_{n+j-1}(t), \tag{3}$$

where $\Delta v_{n+j-1} = v_{n+j} - v_{n+j-1}$ is the velocity difference between car $n+j-1$ and its preceding car $n+j$, p and q are the numbers of preceding cars considered, $\kappa_j = \lambda_j/\tau$, $(j = 1, 2, \ldots, q)$ is the sensitivity of velocity difference. Apparently, the MHVD model is simplified into the OV model for $p = 1$ and $q = 0$. Similarly,[12] the optimal velocity function $V(\cdot)$ depending on the headways is

$$V(\Delta x_n(t), \Delta x_{n+1}(t), \ldots, \Delta x_{n+p-1}(t)) = V\Big(\sum_{l=1}^{p} \beta_l \Delta x_{n+l-1}(t)\Big), \tag{4}$$

where $\beta_l > 0$ $(l = 1, 2, \ldots, p)$ is the weighted function of Δx_{n+l-1}. λ_j decreases with the increase of j, and β_l decreases with the increase of l, which means the effect of ITS information decreases with the increase of preceding car number. Generally, p is equal to q. In this paper, we set $p = q = 3$, $\beta_1 = 6/7$, $\beta_2 = 6/7^2$, $\beta_3 = 1/7^2$, $\lambda_1 = 0.4$, $\lambda_2 = 0.08$, and $\lambda_3 = 0.016$.

2.3. Rules for merging

The rules for merging cars from an on-ramp to the main road are presented in this subsection. For convenience, the same rules for merging are applied to both types of cars. In real traffic, the drivers on an on-ramp consider local traffic condition on the main road, and then determine whether to enter or not. In our simulations, cars on an on-ramp will change to the main road as long as the safety conditions are satisfied. Namely, if the following conditions are fulfilled

$$x_{m1} < x_r(t) < x_{m2} \quad \text{and} \quad d_{\mathrm{of}} > s_{\mathrm{f}} \cdot d_{\mathrm{safe}} \quad \text{and} \quad d_{\mathrm{ob}} > s_{\mathrm{b}} \cdot d_{\mathrm{safe}}, \tag{5}$$

the cars will change from the on-ramp to the main road. $x_r(t)$ is the position of car r on the on-ramp at time t, x_{m1} and x_{m2} are the positions of start and end of section C1, d_{of} denotes the gap between car r and its preceding car on main road, d_{ob} denotes the gap between car r and its nearest following car on the main road, d_{safe} represents the expected safety distance, s_{f} and s_{b} are the safety coefficients. Condition $x_{m1} < x_r(t) < x_{m2}$ means that the car r is on section C1. $d_{\mathrm{of}} > s_{\mathrm{f}} \cdot d_{\mathrm{safe}}$ and $d_{\mathrm{ob}} > s_{\mathrm{b}} \cdot d_{\mathrm{safe}}$ are safety criteria to ensure that no traffic accident occurs. The lane changing rules are asymmetrical, and the lane changing from section C to section C1 is forbidden.

3. Simulations and results

In this section, the effect of ITS information on traffic system near an on-ramp is investigated. The simulation is carried out in an on-ramp system as shown in Fig. 1. The lengths of the sections are $L_{\mathrm{A}} = 2000$ m, $L_{\mathrm{B}} = 1000$ m, $L_{\mathrm{B}} = L_{\mathrm{C1}} = 300$ m, and $L_{\mathrm{D}} = 700$ m. The parameters of the model are set as follows: $a = 1.0$, $d_{\mathrm{safe}} = 10$, $s_{\mathrm{f}} = 0.5$, and $s_{\mathrm{b}} = 0.8$. The open boundary conditions are used in the simulations. If the position of the last car x_{last} exceeds $x = 10$ $(x = 20)$, a car with velocity $V(x)$ enters the main road (on-ramp lane) with inflow rate p_{em} (p_{er}). And the proportion of cars with ITSs is p_{a}. The Euler formats of Eqs. (1) and (3) are employed in numerical simulations. The time step is 0.1 s. The simulation lasts 6000 s and the first 4000 s are discarded to avoid transient behaviours. The flux is obtained by averaging over 2000 s.

3.1. Characteristic of traffic flow consisting of cars without ITSs

In order to investigate the effect of ITS information on the traffic flow near an on-ramp, the characteristic of traffic flow for $p_{\mathrm{a}} = 0$ is studied first. Figure 2 shows the relationship between the flux q_m on section A and the inflow rates p_{em} and p_{er}. It can be seen that the flux q_m increases continuously with p_{em} at very small p_{er}. Then, at appropriate p_{er}, a critical value $p_{\mathrm{em}}^{\mathrm{c}}$ appears on the flux curves, which divides the flow into two regions, i.e. free flow and congested flow. With the increase of p_{em}, q_m increases linearly until $p_{\mathrm{em}}^{\mathrm{c}}$ is reached, and then kept at constant value q_m^{c}. With p_{er} increasing, critical values q_m^{c} and $p_{\mathrm{em}}^{\mathrm{c}}$ become smaller and smaller, and they do not vary when $p_{\mathrm{er}} > 0.15$.

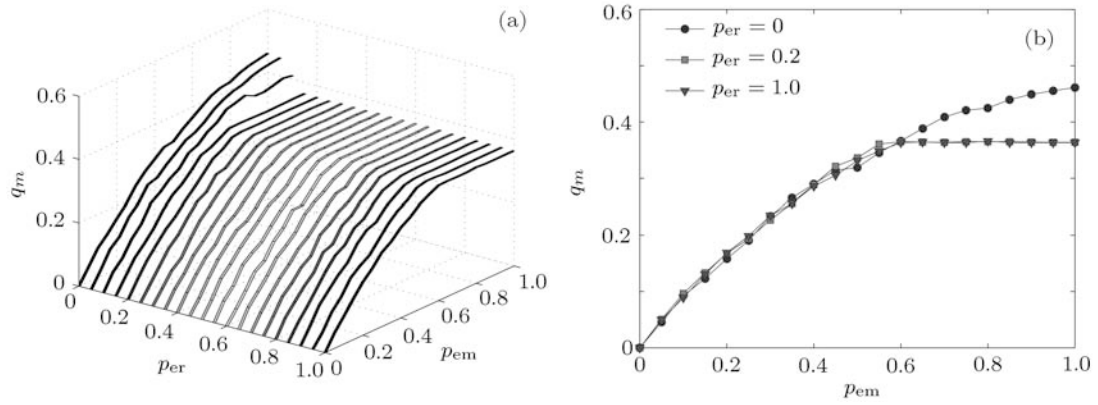


Fig. 2. (a) Variations of flux q_m on section A with inflow rates p_{em} and p_{er} at $p_a = 0$; (b) variations of flux q_m on section A with inflow rate p_{em} at some values of p_{er}.

Figure 3 shows the relationships between the flux q_r on section B (on-ramp flow) and the inflow rates. Similar to the behaviour in Fig. 2, q_r increases continuously with the increase of p_{er} at very small p_{em}. As p_{em} reaches an appropriate value, critical value p_{er}^c appears, and it divides the flow into free flow and congested flow. With the increase of p_{em}, p_{er}^c and the corresponding saturated flux q_r^c decrease, and they keep constant when $p_{em} > 0.6$.

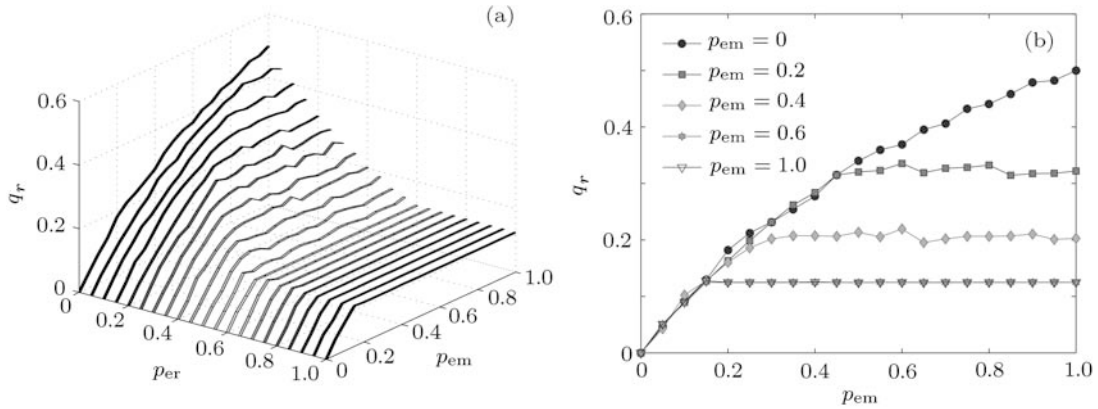


Fig. 3. (a) Variations of flux q_r on section B with inflow rates p_{em} and p_{er} at $p_a = 0$; (b) variations of flux q_r on section B with inflow rate p_{er} at some values of p_{em}.

Figure 4 shows the relationships between flux $q_s = q_m + q_r$ on section C and two inflow rates separately. It can be seen that there is a critical point p_{em}^{sc} (p_{er}^{sc}) which divides the flux curve into two parts. When inflow rate p_{er} (p_{em}) is fixed, the flux q_s increases linearly with the increase of p_{em} (p_{er}) when $p_{em} < p_{em}^{sc}$ ($p_{er} < p_{er}^{sc}$), and q_s reaches maximal value q_s^{max} and keeps constant when $p_{em} > p_{em}^{sc}$ ($p_{er} > p_{er}^{sc}$).

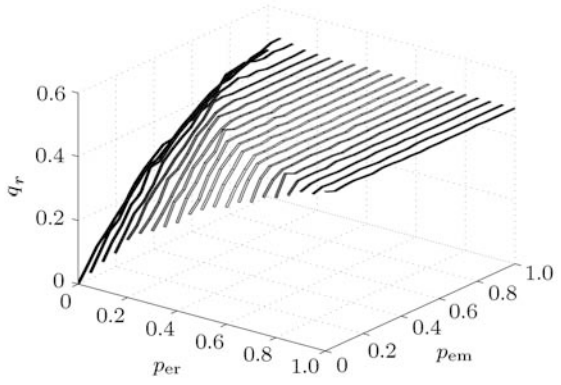


Fig. 4. Variations of flux $q_s = q_m + q_r$ with inflow rates p_{em} and p_{er} at $p_a = 0$.

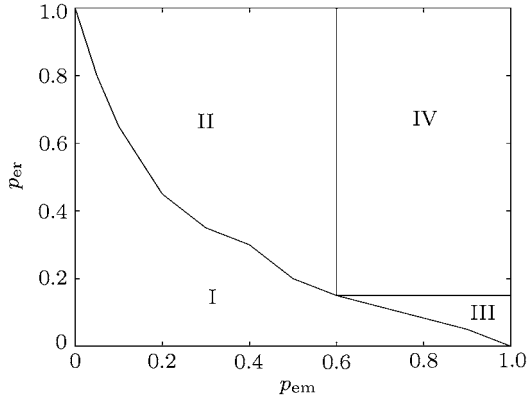


Fig. 5. Phase diagram in space (p_{em}, p_{er}) at $p_a = 0$.

The flows on both section A (main road upstream of the merging region) and section B (on-ramp) have the transition from free flow to congested flow. According to the critical values of $p_{\rm em}^{\rm c}$ and $p_{\rm er}^{\rm c}$, the phase diagram in space ($p_{\rm em}$, $p_{\rm er}$) can be plotted in Fig. 5. From the figure, it can be seen that four regions can be categorized. In order to understand the properties of traffic flow clearly, spatiotemporal diagrams for each region are shown in Figs. 6–9.

In region I, traffic flows on both section A and section B are free flows. From Fig. 6, it can be seen that cars change from section C1 (on-ramp) to section C (main road) almost freely. Interference suffered by the cars on section C is so slight that it can be ignored. Therefore, both the traffic flows are free, and the flux on section A (section B) increases linearly with the increase of inflow rate $p_{\rm em}$ ($p_{\rm er}$) in this region.

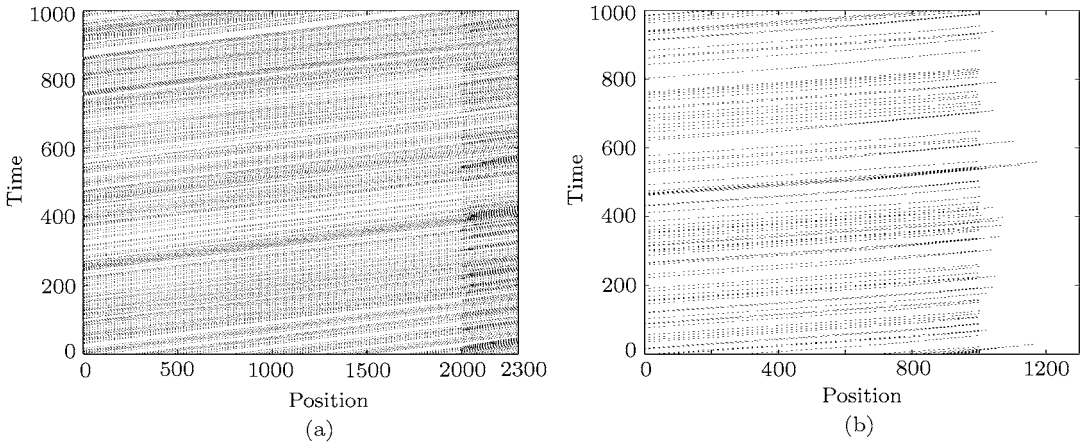


Fig. 6. Spatiotemporal diagrams for $p_{\rm em} = 0.3$ and $p_{\rm er} = 0.1$. (a) main road (sections A and C), where merging region C ranges from location 2000 to 2300; (b) on-ramp, where section C1 ranges from the position 1000 to 1300.

In region II, the traffic is free on section A and it is congested on section B. Figure 7 shows a typical spatiotemporal pattern in this region. One can see that the traffic flow is stable on section A, and the interference on section C can be ignored. However, due to the large inflow rate $p_{\rm er}$, gaps between cars on section C are not sufficient for all the cars on section C1 to change lanes freely. Some cars stop on section C1 and wait for opportunities to enter the main road. Traffic jams appear and propagate upstream on section B (Fig. 7(b)). Thus, the flux on section A increases linearly with $p_{\rm em}$ and is independent of $p_{\rm er}$. The flux on section B does not change with the value of $p_{\rm er}$ and decreases with the increase of $p_{\rm em}$.

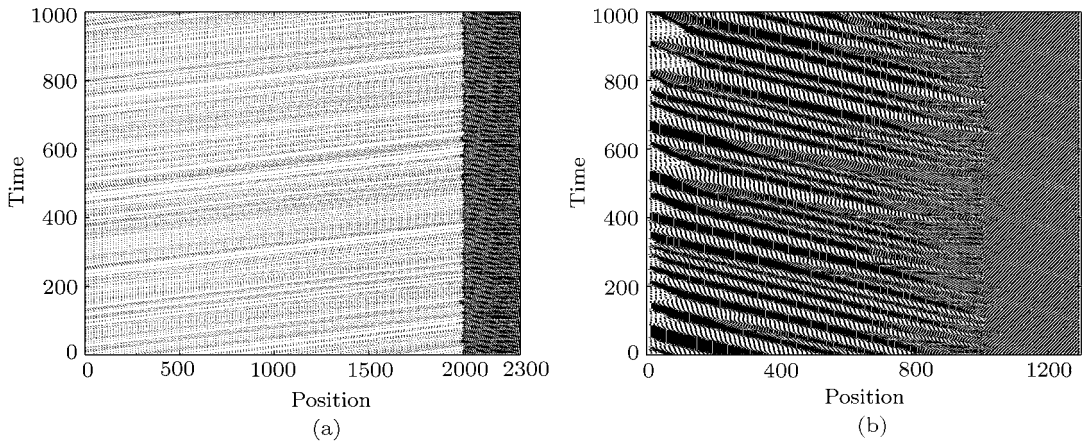


Fig. 7. Spatiotemporal diagrams for $p_{\rm em} = 0.3$ and $p_{\rm er} = 0.6$. (a) Main road; (b) on-ramp.

In region III, the traffic flow on section A is congested, and it is free on section B. Inflow rate $p_{\rm em}$ is large, and the interference between cars in the merging region is serious. Therefore, traffic jams propagate upstream

on section A (Fig. 8(a)). However, inflow rate $p_{\rm er}$ is small, the cars on section C1 can find chances to enter the main road without delay. No jams appear and the traffic flow on section B is free (Fig. 8(b)). Thus, the flux on section A keeps constant with $p_{\rm em}$ and decreases with the increase of $p_{\rm er}$.

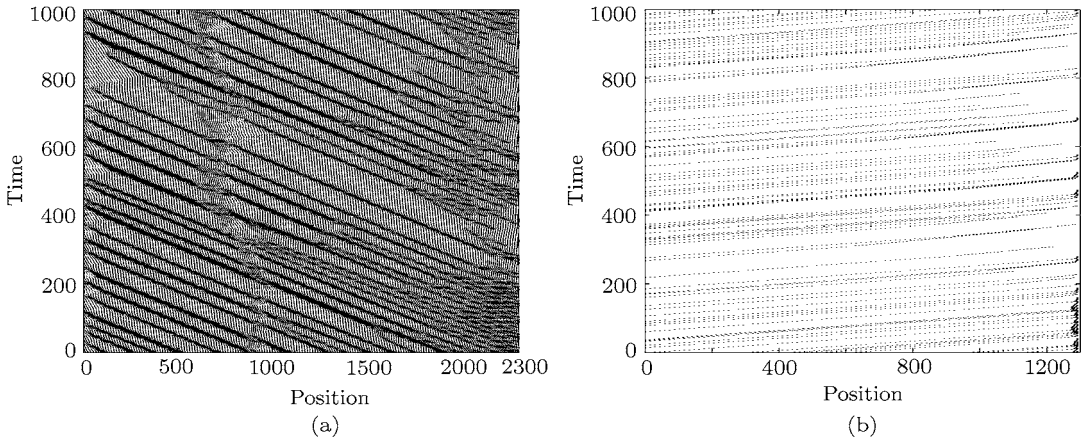


Fig. 8. Spatiotemporal diagrams for $p_{\rm em} = 0.9$ and $p_{\rm er} = 0.1$. (a) Main road; (b) on-ramp.

In region IV, the traffic flows on both section A and section B are congested (Fig. 9). Due to the large inflow rates $p_{\rm em}$ and $p_{\rm er}$, the gap between cars on section C is not sufficient for the entering cars, and the interference in the merging region (section C) is serious. Traffic jams propagate upstream on section A, and the queue of waiting cars reaches the start of section B. Both the fluxed on sections A and B are independent of the inflow rate.

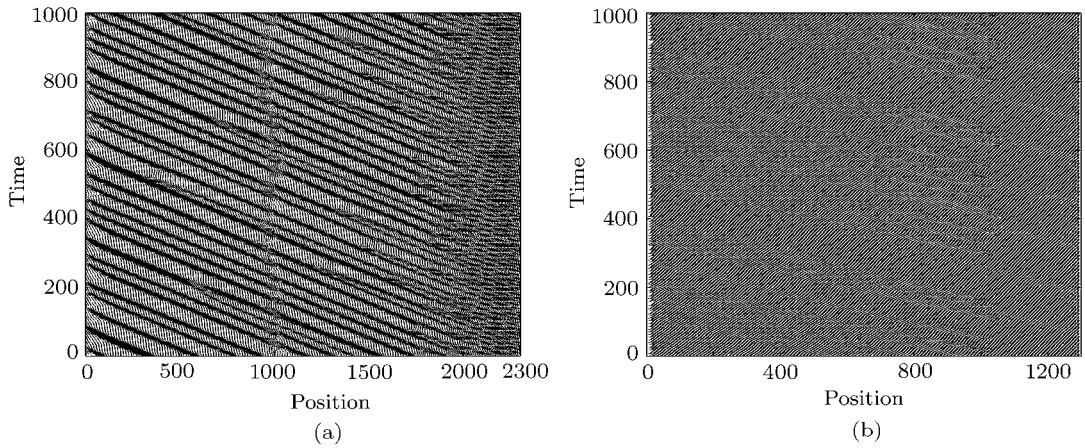


Fig. 9. Spatiotemporal diagrams for $p_{\rm em} = 0.9$ and $p_{\rm er} = 0.6$. (a) main road; (b) on-ramp.

3.2. Characteristics of mixed traffic flows consisting of cars with and without ITSs

Simulations for mixed traffic flow consisting of cars with and without ITSs are carried out in this subsection. Figure 10 shows the relationships between flux and inflow rate at some values of $p_{\rm a}$ (the proportion of cars with ITSs). Figure 10(a) shows the variation of q_m on section A with $p_{\rm em}$ at $p_{\rm er} = 1.0$. It can be seen that each curve has a critical point $p_{\rm em}^{\rm c}$. Critical value $p_{\rm em}^{\rm c}$ increases with the increase of $p_{\rm a}$, and also the corresponding saturated flux increases gradually. Figure 10(b) shows flux q_r on section B as a function of $p_{\rm er}$ at $p_{\rm em} = 1.0$. Similarly, there is a critical point $p_{\rm er}^{\rm c}$ on each curve. However, $p_{\rm er}^{\rm c}$ and the corresponding saturated flux decrease as $p_{\rm a}$ increases. Intuitively, these curves can be explained as follows. With the increase of $p_{\rm a}$, traffic flow on the main road becomes stabler, and the variation of headway becomes smaller. Therefore, it is more difficult for merging cars from the on-ramp. Traffic flow on the main road is improved, while it becomes more serious on the on-ramp lane.

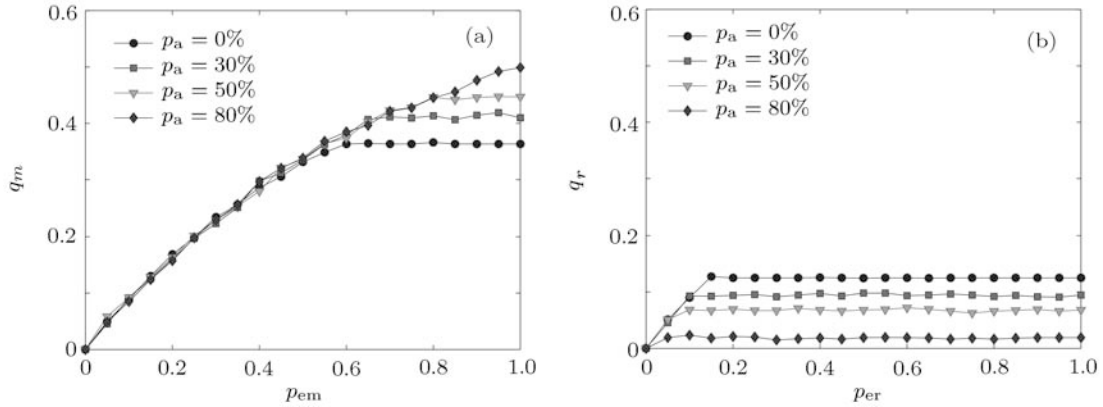


Fig. 10. (a) Variations of flux q_m on section A with inflow rate p_{em} at $p_{er} = 1.0$; (b) variations of flux q_r on section B with inflow rate p_{er} at $p_{em} = 1.0$.

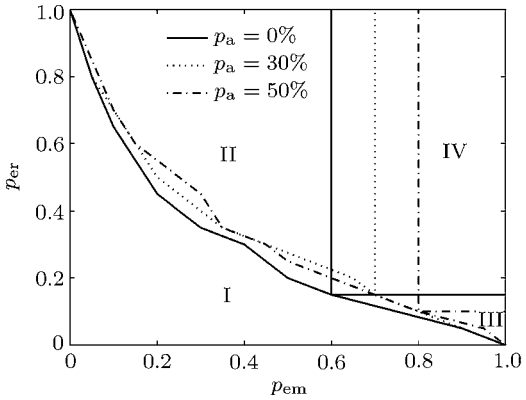


Fig. 11. Phase diagram in space (p_{em}, p_{er}) at some values of p_a.

Figure 11 shows the phase diagrams in space (p_{em}, p_{er}) for $p_a = 0\%$, 30% and 50%. Similar to the diagrams in Fig. 5, the diagrams in Fig. 11 are classified into four regions. In region I, traffic flows on both section A and section B are free flows. In region II, traffic is free on section A, and it is congested on section B. Oppositely, in region III, traffic flow is congested on section A and it is free on section B. Both the traffic flows are congested in region IV. As p_a increases, regions I and II are enlarged while regions III and IV shrink gradually. When $p_a > 80\%$, regions III and IV completely disappear, and only regions I and II survive (Fig. 12). Accordingly, flux q_m on section A increases linearly with the increase of p_{em} and it is independent of p_{er} (Fig. 13(a)). And as p_{em} increases, the critical value and the corresponding saturated flux on section B decrease continuously (Fig. 13(b)).

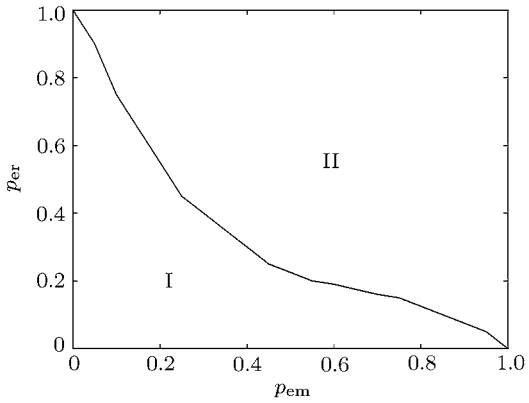


Fig. 12. Phase diagram in space (p_{em}, p_{er}) at $p_a = 80\%$.

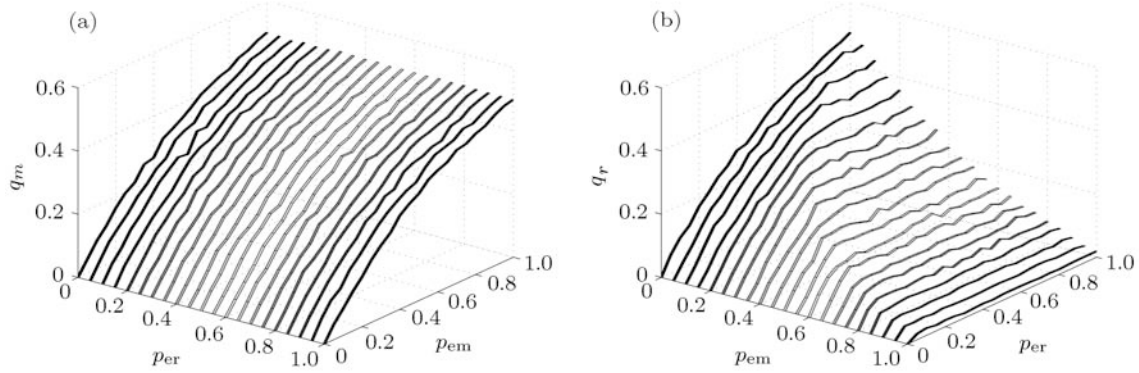


Fig. 13. Variations of flux (a) q_m on section A and (b) q_r on section B with inflow rates p_{em} and p_{er} for $p_a = 80\%$.

Figure 14 shows the spatiotemporal diagrams for $p_{\rm em} = 0.9$ and $p_{\rm er} = 0.6$ with $p_{\rm a} = 50\%$. Comparing Fig. 9(a) (for the case without ITS) with Fig. 14(a) (for the case with ITS), one can see that traffic jams on the main road are suppressed to a great extent by using the ITS information, and the traffic flow becomes stabler. However, traffic congestion on the on-ramp lane is still serious (Fig. 14(b)).

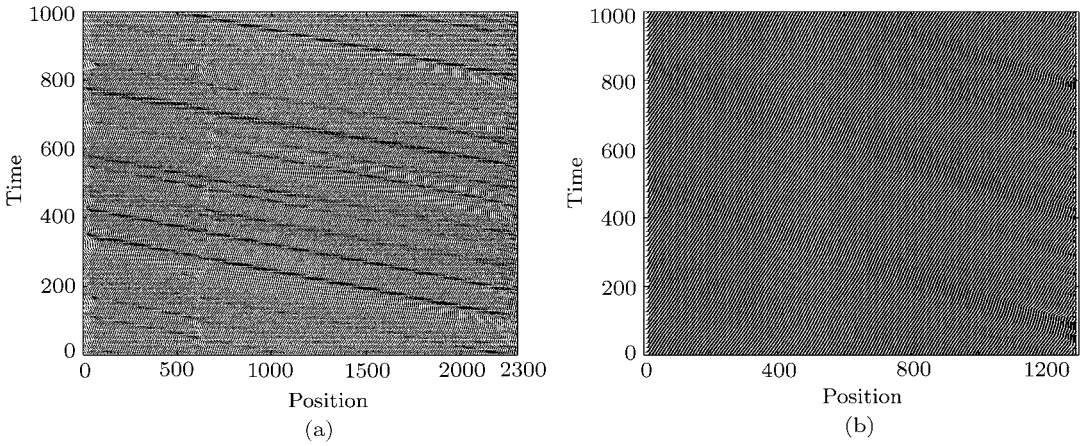


Fig. 14. Spatiotemporal diagrams for $p_{\rm em} = 0.9$ and $p_{\rm er} = 0.6$ with $p_{\rm a} = 50\%$. (a) Main road; (b) on-ramp.

To understand the effect of ITS information on flux and phase transitions of traffic flow near the on-ramp, the headways and velocities for cars on the main road are displayed in Figs. 15 and 16.

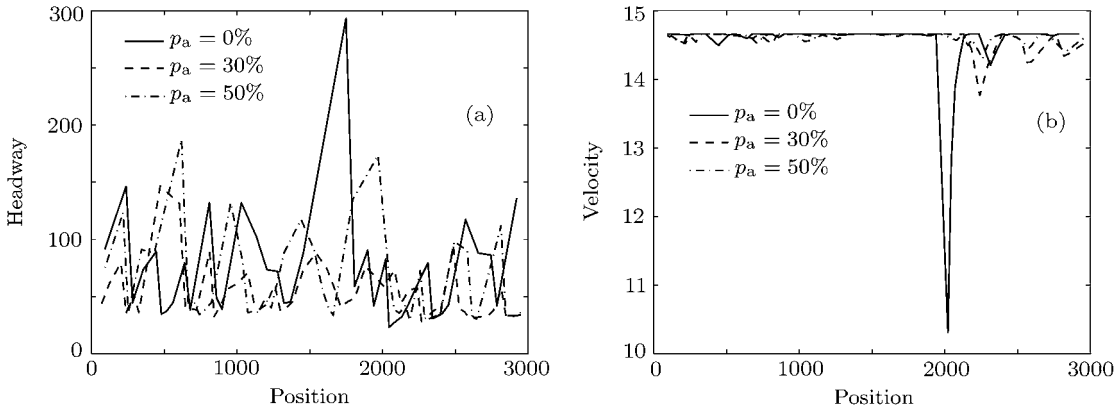


Fig. 15. (a) Headways and (b) velocities for $p_{\rm em} = 0.3$, $p_{\rm er} = 0.1$, and three different values of $p_{\rm a}$ at $t = 5000$ s.

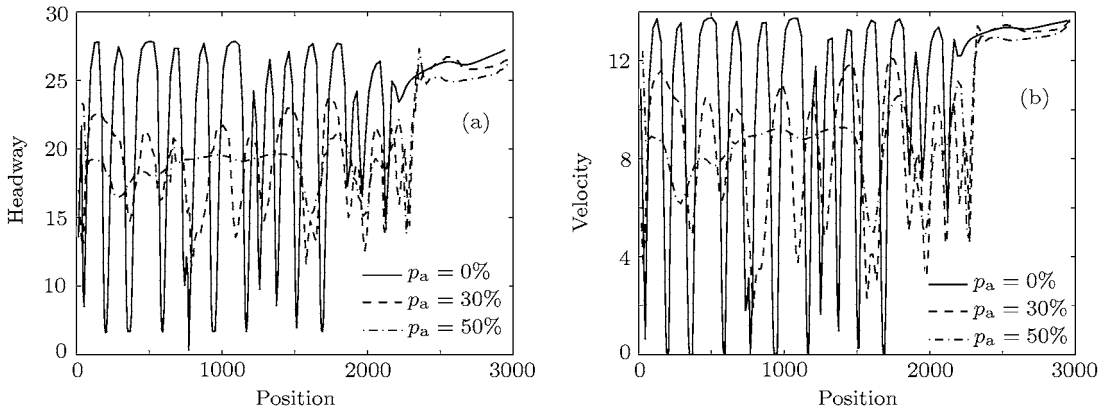


Fig. 16. (a) Headways and (b) velocities for $p_{\rm em} = 0.9$, $p_{\rm er} = 0.1$, and three values of $p_{\rm a}$ at $t = 5000$ s.

Figure 15 shows the headways and velocities for $p_{\rm em} = 0.3$, $p_{\rm er} = 0.1$, and three different values of $p_{\rm a}$ at $t = 5000$ s. The traffic flow is free on section A, the headway for each car is larger than 40 (Fig. 15(a)) and cars move freely with their maximum velocities (Fig. 15(b)). The fluctuation of velocity in merging region disappears along the downstream of the road, and the amplitude of fluctuation becomes smaller with the increase of $p_{\rm a}$. Similar results can be found in the case of congested traffic on section A (Fig. 16). With the increase of $p_{\rm a}$, the fluctuations of headway and velocity become smaller (Figs. 16(a) and 16(b)), the stability of traffic flow is enhanced, and so the number of gaps available for merging lessens according to Eq. (5). Therefore, for section A, the saturated flux increases and the free flow region is enlarged with the increase of $p_{\rm a}$. Contrarily, for section B, the saturated flux decreases and the free flow region shrinks as $p_{\rm a}$ increases.

Finally, the effect of ITS information on the capacity of the on-ramp system is investigated. In this work, the maximal capacity of the system is defined as

$$q_s^{\max} = \max(q_m + q_r). \tag{6}$$

Namely, the capacity is the maximal flux that the system can afford. Figure 17 shows the relationship between capacity $q_s^{\max}$ and $p_{\rm a}$. It can be found that there

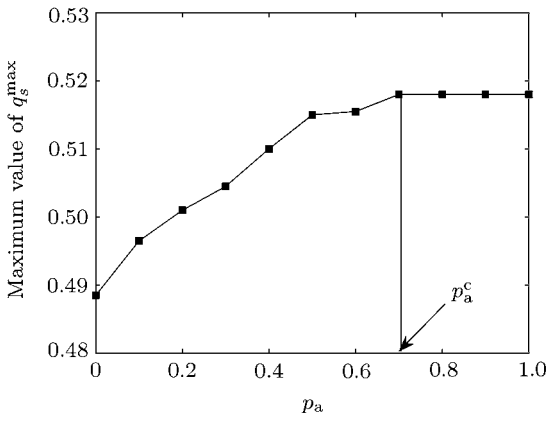


Fig. 17. Variation of capacity $q_s^{\max}$ with $p_{\rm a}$.

is a critical point $p_{\rm a}^{\rm c}$ on the curve. $q_s^{\max}$ increases with $p_{\rm a}$ when $p_{\rm a} < p_{\rm a}^{\rm c}$, and it keeps constant when $p_{\rm a} > p_{\rm a}^{\rm c}$. Compared with the capacity in the system without ITS information, the capacity in the system with ITS is promoted by 13% when $p_{\rm a} > p_{\rm a}^{\rm c}$. The results indicate that the capacity of the on-ramp system can be promoted by introducing the ITS, although the capacity of the on-ramp lane is reduced. As a result, a controlling method can be presented by adjusting the proportion of cars with ITSs in an appropriate region, where the capacity is promoted and the flux on the on-ramp does not decrease too much.

4. Conclusions

The present work addresses the effect of cars with intelligent transportation systems (ITSs) near an on-ramp system. The optimal velocity (OV) model and multiple headway and velocity difference (MHVD) model are used to depict the dynamics of cars with and without ITS, respectively. Numerical simulations are performed to investigate the characteristic of traffic flow near an on-ramp. The results show that both the flux and the phase diagrams can be classified into two types according to the proportion $p_{\rm a}$ of cars with ITSs. At small $p_{\rm a}$, the traffic flows on both section A (upstream of the merging region) and section B (on-ramp lane) can be divided into free flow and congested flow by the critical values of inflow rates. According to the critical values, the phase diagram is plotted in space $(p_{\rm em}, p_{\rm er})$. It is found that four regions can be categorized.

As $p_{\rm a}$ increases, traffic flow becomes more and more stable, and the number of mainline gaps available for merging becomes less. Therefore, the saturated flux for section A increases and the free flow region is enlarged. Contrarily the saturated flux for section B decreases and the free flow region shrinks. When $p_{\rm a} > 80\%$, the traffic on section A is free in the regions of whole phase diagram. Only two regions can be classified according to the traffic state of section B.

The capacity of the on-ramp system is investigated, too. The results indicate that the capacity of the on-ramp system can be promoted by introducing the ITS, although the capacity of the on-ramp lane is reduced.

References

[1] Chowdhury D, Santen L and Schadschneide A 2000 *Phys. Rep.* **329** 199

[2] Helbing D 2001 *Rev. Mod. Phys.* **73** 1067

[3] Bando M, Hasebe K, Nakayama A, Shibata A and Sugiyama Y 1995 *Phys. Rev.* E **51** 1035

[4] Helbing D and Tilch B 1998 *Phys. Rev.* E **58** 133
[5] Jiang R, Wu Q S and Zhu Z J 2001 *Phys. Rev.* E **64** 017101
[6] Xue Y, Dong L Y, Yuan Y W and Dai S Q 2002 *Acta Phys. Sin.* **51** 492 (in Chinese)
[7] Xue Y 2003 *Acta Phys. Sin.* **52** 2750 (in Chinese)
[8] Nagatani T 1999 *Phys. Rev.* E **60** 6395
[9] Nakayama A, Sugiyama Y and Hasebe K 2001 *Phys. Rev.* E **65** 016112
[10] Lenz H, Wagner C K and Sollacher R 1999 *Eur. Phys. J.* B **7** 331
[11] Hasebe K, Nakayama A and Sugiyama Y 2003 *Phys. Rev.* E **68** 026102
[12] Ge H X, Dai S Q, Dong L Y and Xue Y 2004 *Phys. Rev.* E **70** 066134
[13] Ge H X, Dai S Q and Dong L Y 2006 *Physica* A **365** 543
[14] Ge H X, Cheng R J and Dai S Q 2005 *Physica* A **357** 466
[15] Wang T, Gao Z Y and Zhao X M 2006 *Acta Phys. Sin.* **55** 634 (in Chinese)
[16] Li Z P and Liu Y C 2006 *Eur. Phys. J.* B **53** 367
[17] Xie D F, Gao Z Y and Zhao X M 2008 *Commun. Comput. Phys.* **3** 899
[18] Kikuchi S, Uno N and Tanaka M 2003 *J. Transp. Eng.* **129** 146
[19] Kerner B S 2003 e-print cond-mat/0309017
[20] Rakha H, Hankey J, Patterson A and Aerde M V 2001 *J. Intell. Transp. Syst.* **6** 225
[21] Li P Y 2002 *Transp. Res. Part* C **10** 275
[22] Yi J G and Horowitz R 2006 *Transp. Res.* Part C **14** 81
[23] Treiber M and Helbing D 2002 e-print cond-mat/0210096
[24] Kesting A, Treiber M, Schönhof M, Kranke F and Helbing D 2006 e-print physics/0601096
[25] Davis L C 2004 *Phys. Rev.* E **69** 066110
[26] Davis L C 2007 *Physica* A **379** 274
[27] VanderWerf J, Shladover S E, Miller M A and Kourjanskaia N 2002 *Transp. Res. Rec.* **1800** 78
[28] Ioannou P A and Stefanovic M 2005 *IEEE Trans. Intell. Transp. Syst.* **6** 79
[29] Xie D F, Gao Z Y and Zhao X M 2008 *Chin. Phys.* B **17** 4440
[30] Chen S D, Zhu L H, Zheng R S, Kong L J and Liu M R 2009 *Acta Phys. Sin.* **58** 2271 (in Chinese)